Electronic Supplementary Material (ESI) for RSC Advances.

Supplementary Material

Selection of highly specific and selective aptamers using modified SELEX and their use in process analytical technique of Lucentis bioproduction

Tanu Bhardwaj[a], Anurag S. Rathore[b], Sandeep Kumar Jha[a]

[a]Centre for Biomedical Engineering, Indian Institute of Technology, Hauz Khas, New Delhi-110016, India.

[b] Department of Chemical Engineering, Indian Institute of Technology, Hauz Khas, New Delhi-110016, India.

Email: sandeepkjha [at] gmail.com

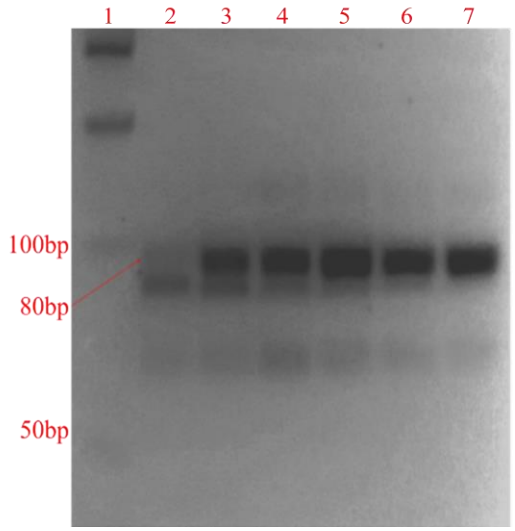

(a)

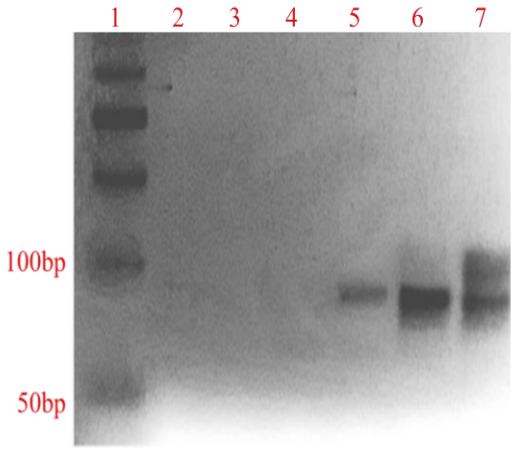

(b)

Fig. S1. (a) Gel electrophoresis of PCR products with different number of PCR cycles (left to right). Lane 1: 50 bp ladder, Lane 2-7: PCR products after 10, 15, 20, 25, 30 and 35 cycles of amplification on 4 % agarose gel. (b) Gel electrophoresis of blank samples with different number of PCR cycles. Lane 1: 50 bp ladder, Lane 2-7: Blank samples after 10, 15, 20, 25, 30 and 35 cycles of amplification on 4 % agarose gel. Comparing (a) and (b), most intense band at 80 bp without non-specific bands was seen with 20 PCR cycles.

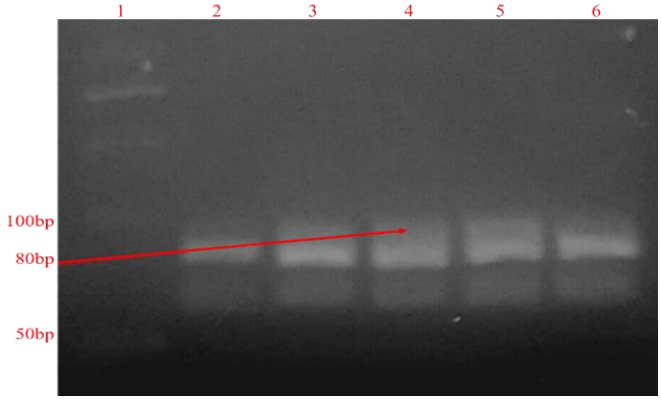

Fig. S2. Gel electrophoretogram showing dsDNA band at 80bp with different annealing temperatures (left to right). Lane 1: 50 bp ladder, Lane 2-6: PCR products with 20 PCR cycles and annealing temperature of 45, 50, 55, 60 and 65 degree Celsius on 4 % agarose gel. Due to absence of non-specific bands in blank samples, gel image is not included here

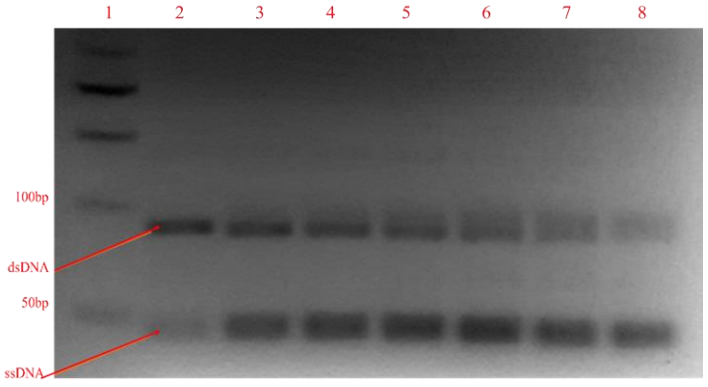

(a)

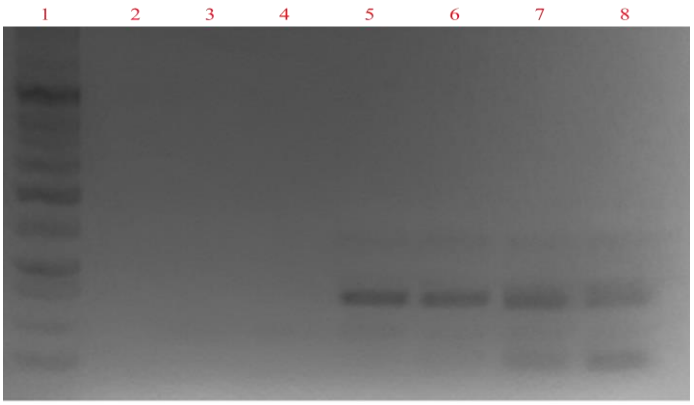

(b)

Fig. S3. (a) Gel electrophoresis of asymmetric PCR products with different number of PCR cycles (left to right). Lane 1: 50 bp ladder, Lane 2-8: asymmetric PCR products with primer ratio 20:1 and different number of PCR cycles 10, 15, 20, 25, 30, 35 and 40 on 4 % agarose gel. (b) Gel electrophoresis of blank samples with different number of PCR cycles. Lane 1: 50 bp ladder, Lane 2-8: Blank samples with primer ratio 20:1 and different number of PCR cycles 10, 15, 20, 25, 30, 35 and 40 on 4 % agarose gel. Comparing (a) and (b), maximum yield of regenerated ssDNA was seen without non-specific bands was seen with 20 PCR cycles

S1. **FTIR study of immobilization of Lucentis on sepharose beads**

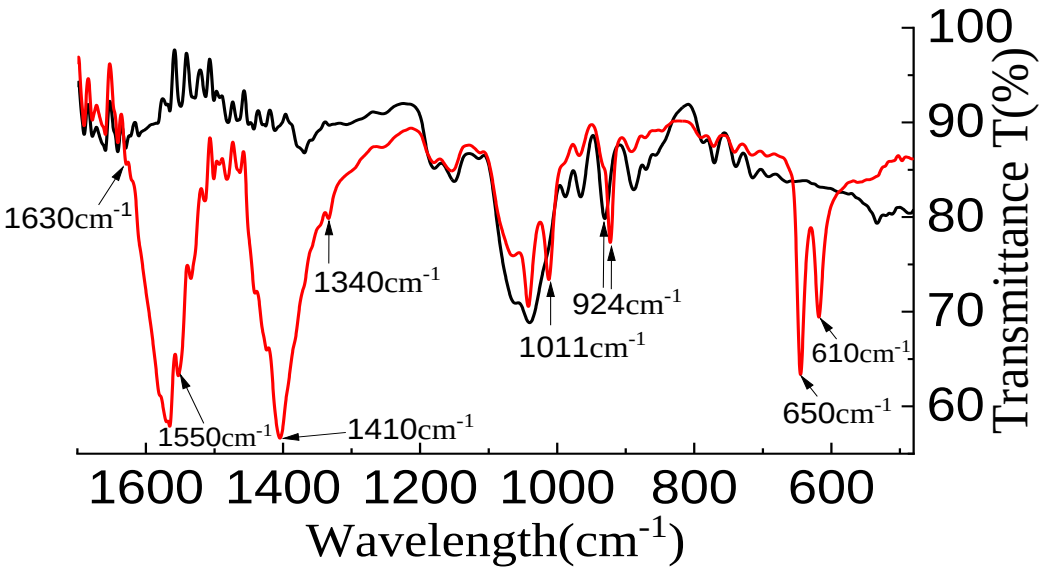

Fig.S4. FTIR spectra of sepharose beads before (———) and after immobilization (———) of Lucentis.

Immobilization of Lucentis on sepharose beads for affinity column chromatography was confirmed using Fourier transform infrared spectroscopy (FTIR). FTIR spectra for sepharose beads before and after immobilization of Lucentis were recorded and are shown in Fig.S4. Primarily, sepharose beads showed their characteristic signature peaks for glycosidic linkage and vibration of C-O-C of 3,6-anhydro- L-galactopyranose at 1011 and 924cm^{-1}.[1] Then, characteristic peaks of protein (Lucentis) were obtained at 1630, 1550 and 1340cm^{-1} for amide I, II and III bonds in addition to $SiCH_2$(1410cm^{-1}) and Si-O-Si (1011cm^{-1}) peaks of (3-Aminopropyl)triethoxysilane (APTES) after immobilization of Lucentis on sepharose beads using APTES and glutaraldehyde.[2, 3] Additionally, intense peaks were seen due to N-H wagging in Lucentis near 600cm^{-1}.[4] These amide peaks altogether with peaks of sepharose supported presence of Lucentis on sepharose beads. Lowry's protein quantitative estimation method also verified immobilization of Lucentis on sepharose beads. In this method, we simply checked the concentration of Lucentis in elutant while filling the column with Lucentis immobilized sepharose beads. It was found out that approximately 80% of Lucentis during immobilization was retained on sepharose beads.

Table S1: Strategy involved in each cycle of SELEX process

Selex cycle	Concentration of immobilized Lucentis (mg)	Incubation time (min)	Volume of washing buffer (ml)	Eluting buffer
1	**2.3**	**60**	**10**	**30 ml 3 M NaCl.**
2	**2.3**	**60**	**20**	**30 ml 3 M NaCl.**
3	**2.3**	**60**	**30**	**30 ml 3 M NaCl.**
4	**0.25**	**30**	**40**	**30 ml 3 M NaCl.**
5	**0.25**	**30**	**60**	**40 ml 3 M NaCl.**
6	**0.25**	**30**	**70**	**50 ml 3 M NaCl and 10 ml 6 M NaCl at 100 ˚C.**
7	**0.1**	**15**	**80**	**60 ml 3 M NaCl and 10 ml 6 M NaCl at 100 ˚C.**
8	**0.1**	**15**	**200**	**100 ml 3 M NaCl, 100 ml basic elution buffer pH 8, 100 ml acidic elution buffer pH 3.6 and 10 ml acetate buffer at 100 ˚C.**
9	**0.1**	**15**	**300**	**200 ml 3 M NaCl, 150 ml basic elution buffer pH 8, 150 ml acidic elution buffer pH 3.6 and 10 ml acetate buffer at 100 ˚C.**
10	**0.1**	**15**	**400**	**300 ml 3 M NaCl, 200 ml basic elution buffer pH 8, 200 ml acidic elution buffer pH 3.6 and 10 ml acetate buffer at 100 ˚C.**

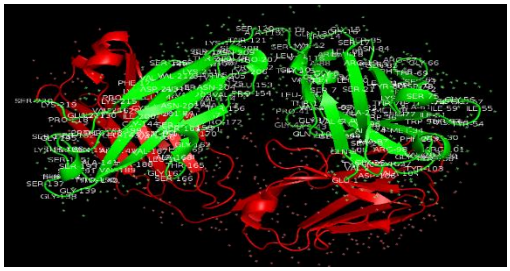

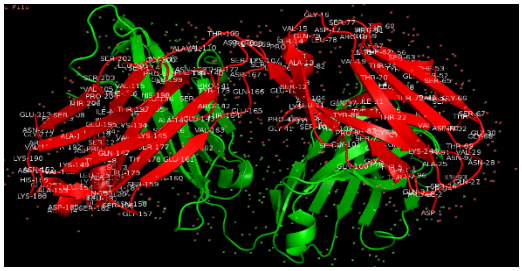

(a) (b)

Heavy chain-aptamer complex Light chain-aptamer complex

Seq 1

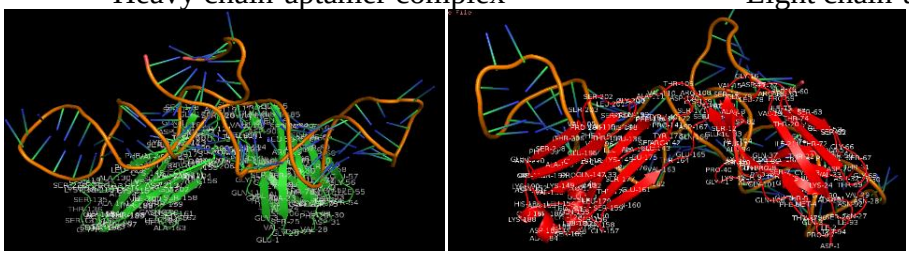

Seq 2

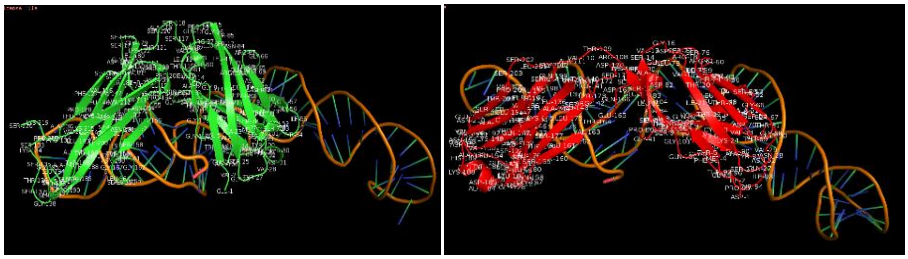

Seq 3

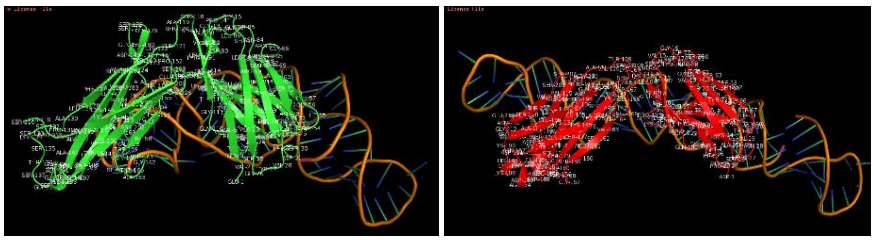

Seq 4

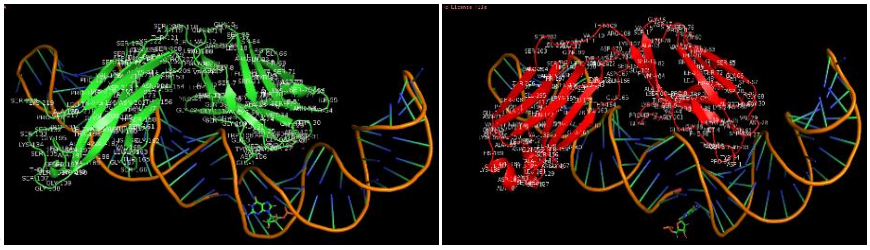

Seq 5

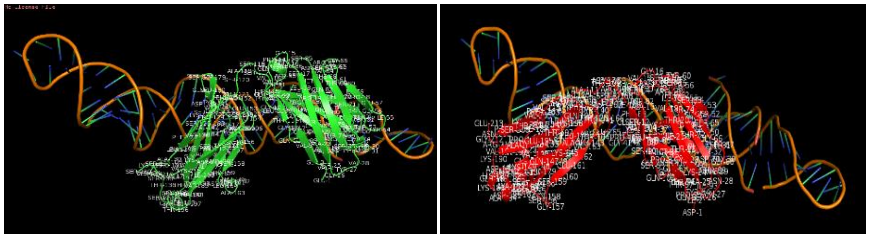

Seq 6

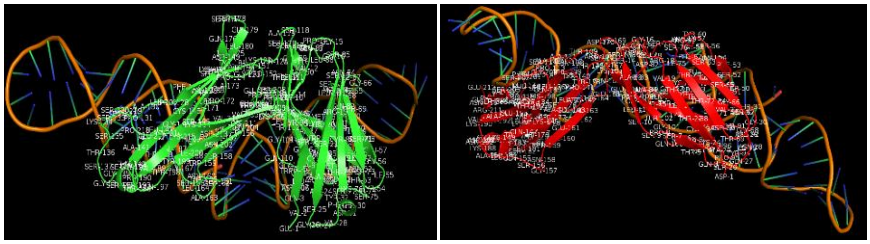

Seq 7

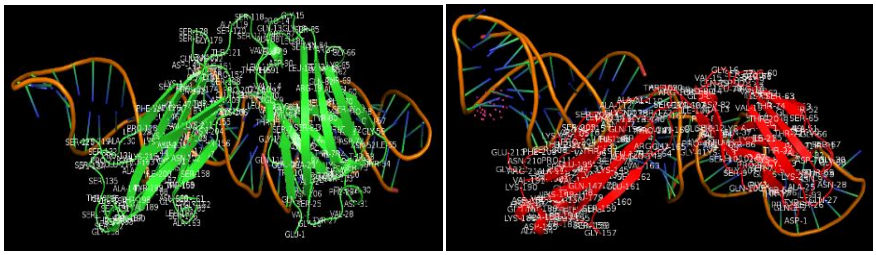

Seq 8

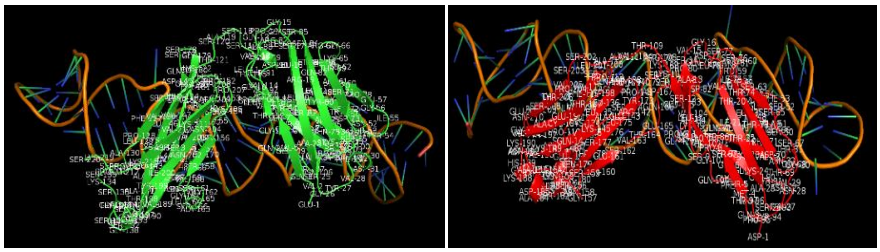

Seq 9

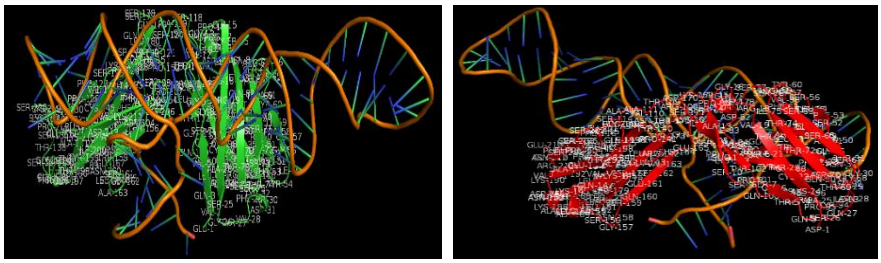

Seq10

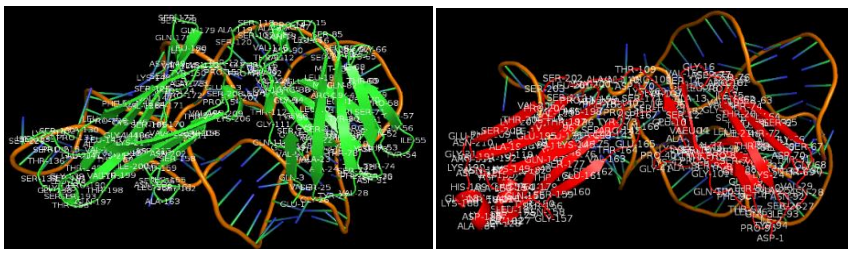

Seq11

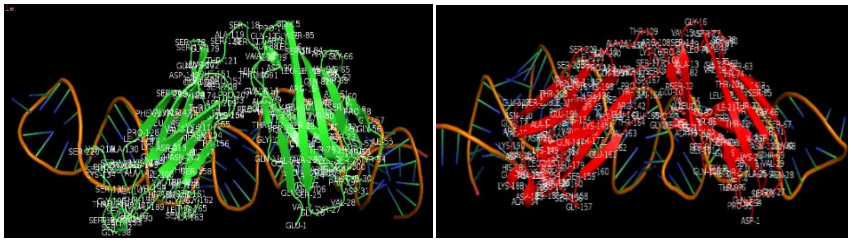

Seq12

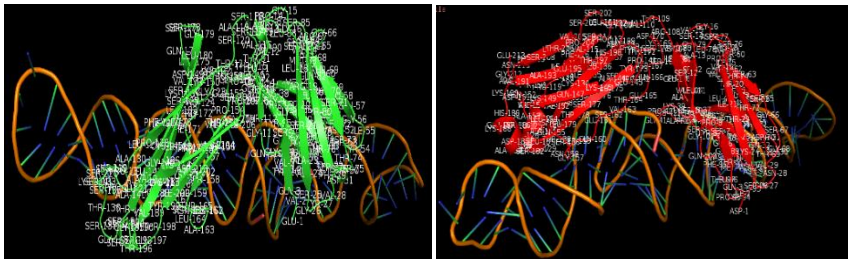

Seq13 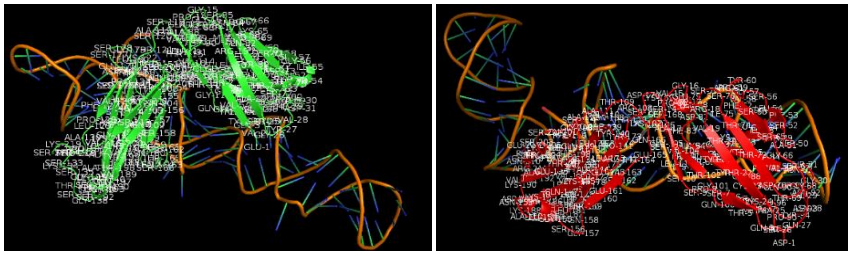

Seq14 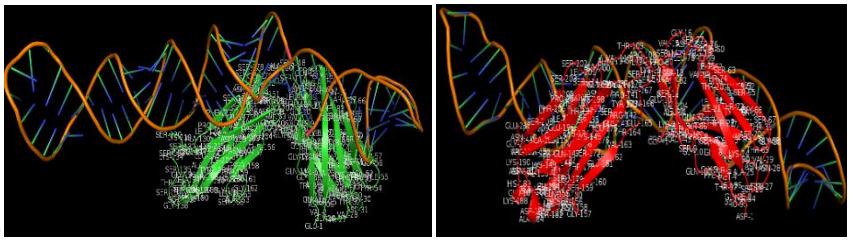

Seq 15 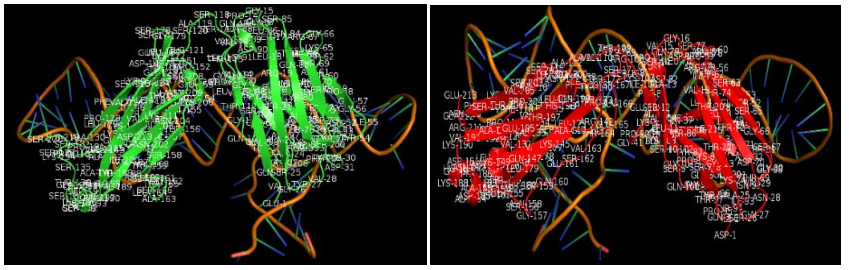

Seq 16 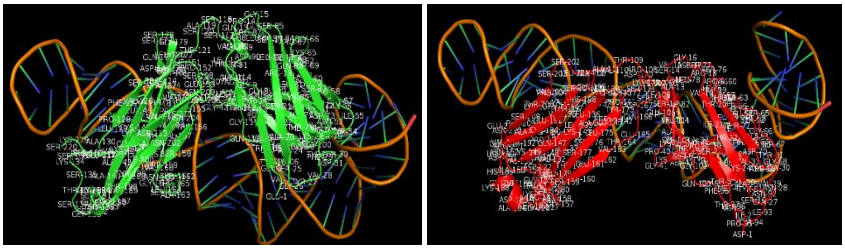

Seq 17 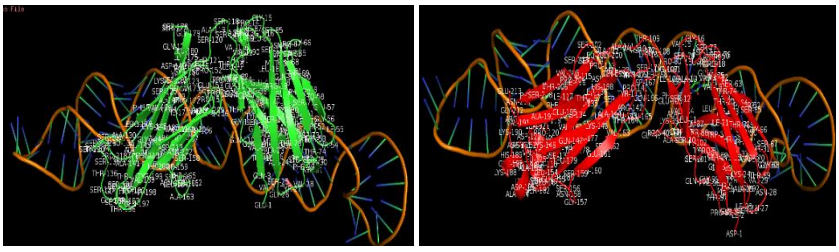

Seq 18 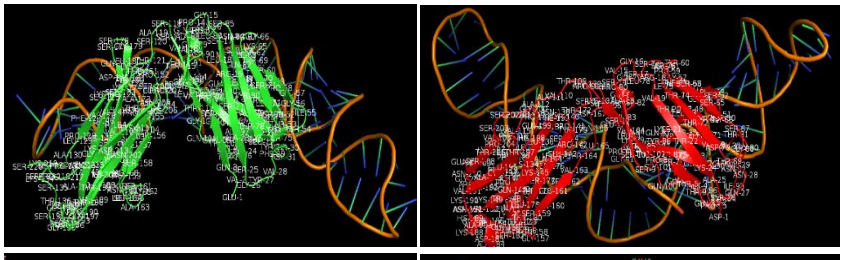

Seq 19 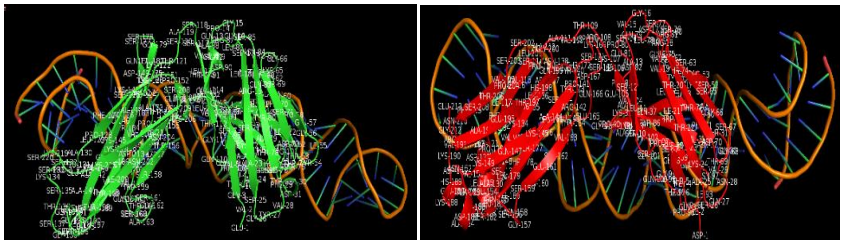

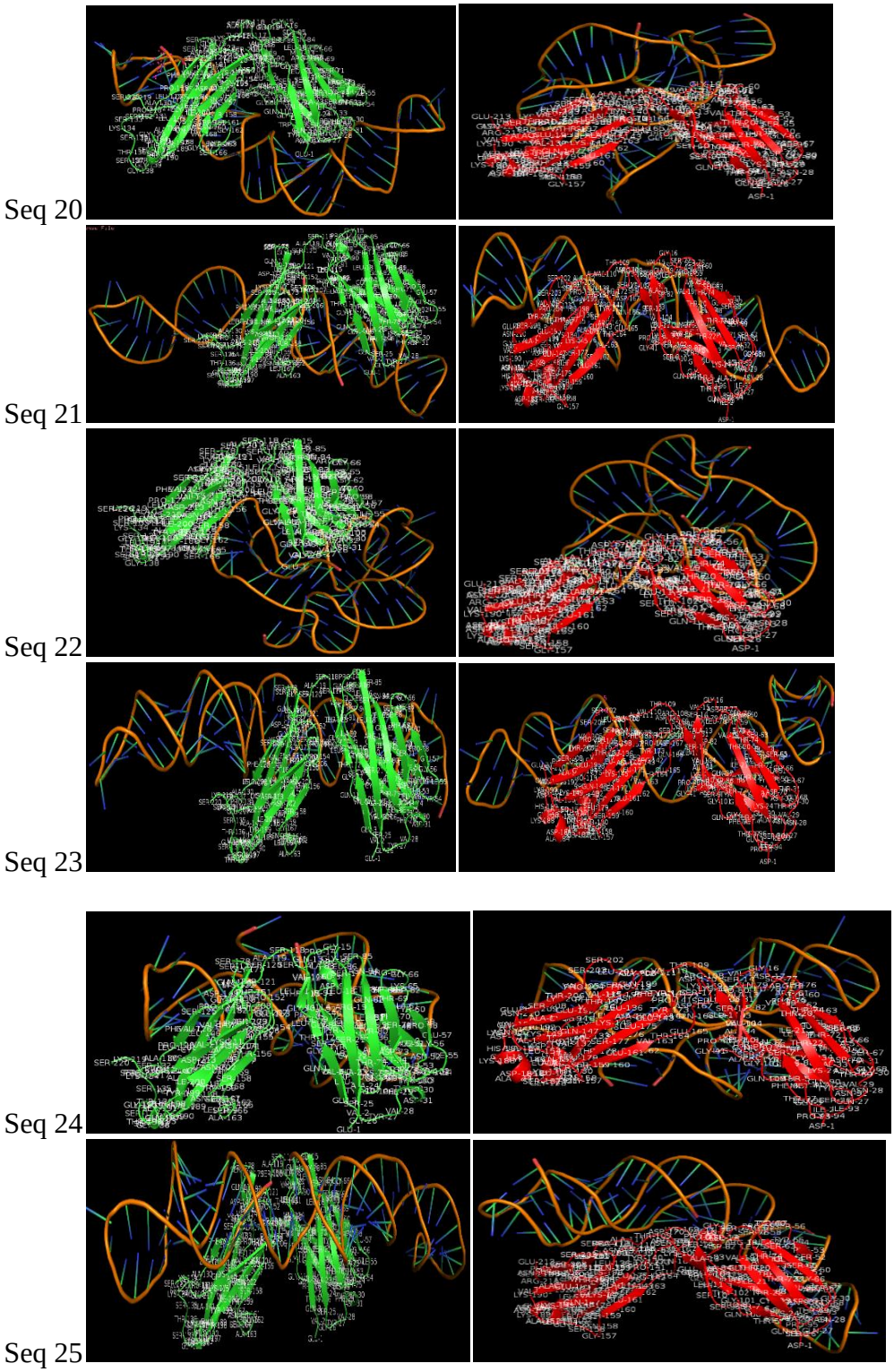

(c)

Fig.S5. Interaction of heavy and light chain of lucentis where (a) heavy chain (green) is kept in front to show that its other (back) side is engaged with light chain (red); (b) light chain (red) interaction is kept in front to show that its other side (back) is engaged with heavy chain (green) in lucentis. Light and heavy chain interacts via their active sites. In both cases (a) and (b), heavy and light chain of lucentis is oriented

in such a way that their active site for the other chain is on back side. This made further comparison of different docking pairs easier visually. Other than this active site are passive sites (front side of heavy chain in (a) and light chain in (b)) where aptamer can bind; (c) Interaction of each sequence with heavy and light chain of lucentis. In all cases, the orientation of both chains is same as it was in (a) and (b), meaning while docking of aptamer with heavy chain of lucentis, the backside is already engaged for interaction with light chain and vice versa. Only those sequences are selected which binds to passive sites (front side).

S2. **Binding assay and calculation of dissociation constant using thermofluorimetric analysis**

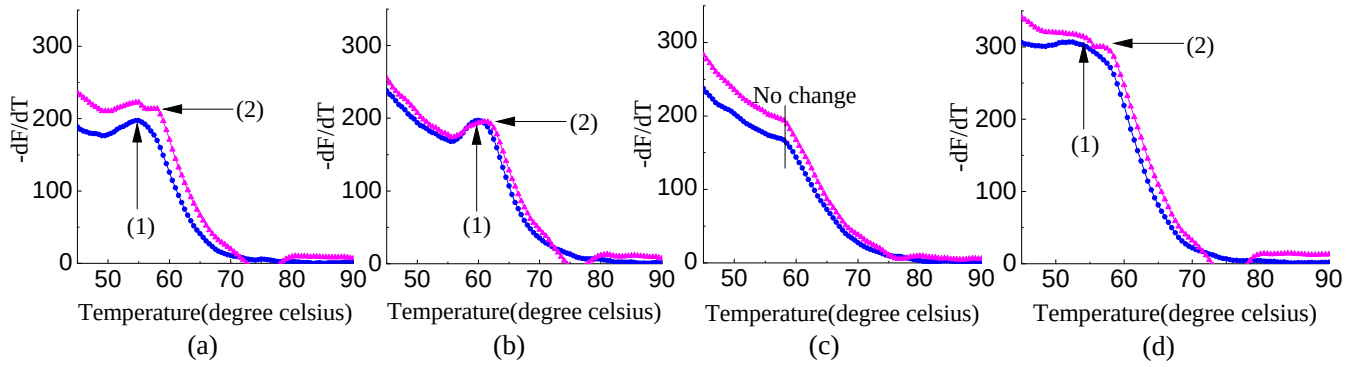

Fig.S6. Aptamer-Lucentis(——) binding studies involving thermofluorimetric analysis of sequence (——): (a) 1 (b) 9 (c) 14 (d) 25 between temperatures 45 to 90 ˚C. Blank readings were subtracted from all the data and then the graphs were plotted. Peak (1) and (2) corresponds to aptamer and aptamer-Lucentis complex respectively

S2: Methodology: In this technique, each of four aptamers was incubated with Lucentis in presence of fluorescent ssDNA binding dye SYBR green II. Reaction mixtures of 50µl were prepared in phosphate buffer pH 5.7 with 100mM KCl with final concentration of 100nM aptamer, 10x SYBR green II and Lucentis. Then, all the reaction mixtures were incubated at 25°C for half an hour and scanned at 0.5°C /min using real-time PCR instrument for measuring fluorescence intensities between 45 to 90°C. Melting temperature for each aptamer sequence and their complex with Lucentis was measured and compared for further selection of best binding affinity aptamer for Lucentis.

Then, best aptamer sequences were used for estimation of K_d via thermofluorimetric analysis at different concentrations of Lucentis, 13.33nM, 33.33nM, 66.66nM, 333.3nM, 666.6nM, 3500nM and 6666nM. The fluorescence intensities for each reaction mixture was measured using real-time PCR and a saturation curve was plotted for calculating K_d. Reactions were carried out in sextuplicates to calculate standard deviation in measurements.

S2: Discussion: In this method, melting peak of aptamer and aptamer-Lucentis complex was recorded using real-time PCR thermal scanning.[5] As after hybridization, due to comparatively higher thermodynamic stability, dsDNA shows melting peak at higher temperature than ssDNA, similar case was with aptamer-protein complex. When the aptamer-Lucentis mixture was scanned in real-time PCR, then generation of a new melting peak at higher temperature than that of aptamer was observed with sequence 1, 9 and 25 as shown in Fig. S6 (a, b and d). This new peak verified formation of thermally stable aptamer-Lucentis complex in the mixture in comparison to aptamer itself and confirmed the affinity of aptamer for Lucentis. Here, more the difference between aptamer and aptamer-Lucentis complex melting peak, higher would be the stability of complex and hence, the affinity of aptamer for Lucentis. In addition, less affinity of aptamer for Lucentis in comparison to other three aptamers as no melting peak was obtained in sequence 14 (Fig.S6 (c)) for aptamer-Lucentis complex. Aptamer 1 and 25 reported maximum difference in temperatures of melting peak, hence, it was further used for estimation of K_d.

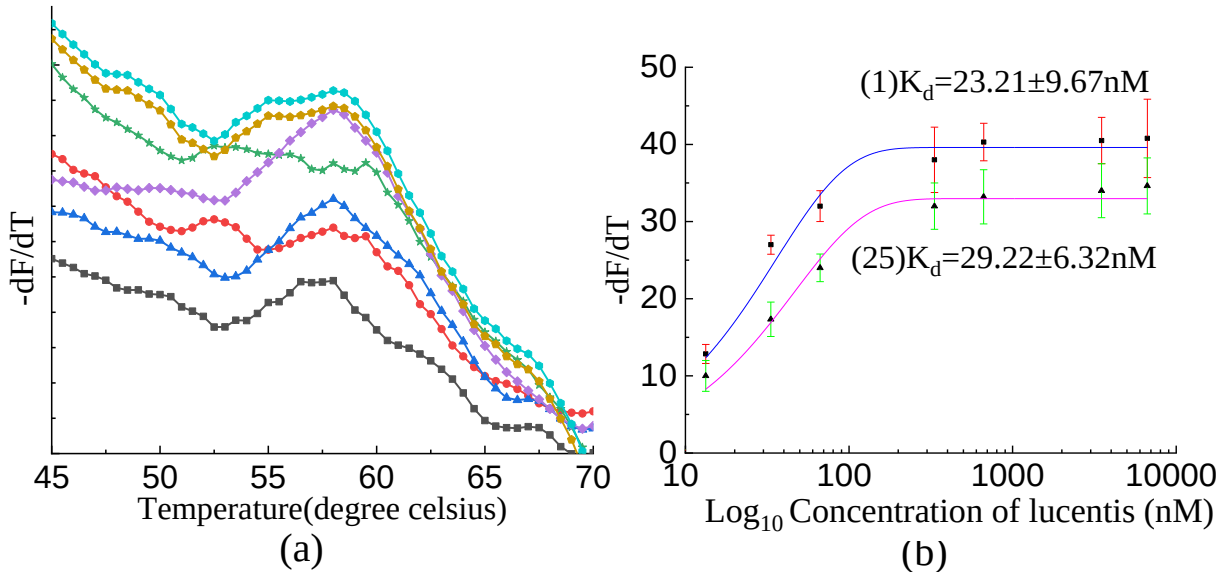

Fig.S7. Dissociation constant studies involving thermofluorimetric analysis with (a) aptamer-1with different concentrations of Lucentis, 13.33 nM (—■—), 33.33 nM (—●—), 66.66 nM (—▲—), 333.3 nM (—★—), 666.6 nM (—◆—), 3500 nM (—●—) and 6666 nM (—●—); (b) calibration curve obtained between –dF/dT versus concentration of Lucentis for aptamer sequence-1(1) and sequence-25(25).

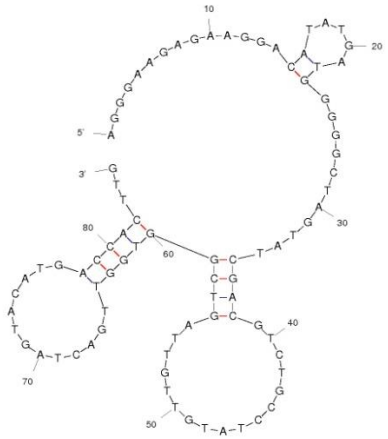

Aptamer 1

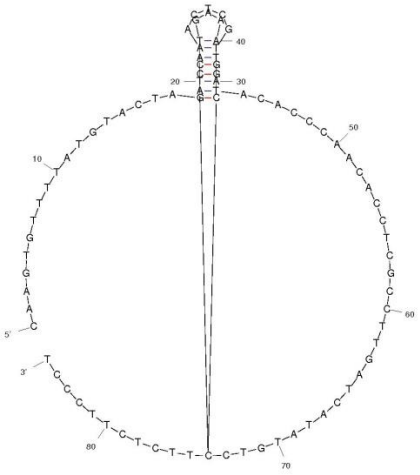

Aptamer 2

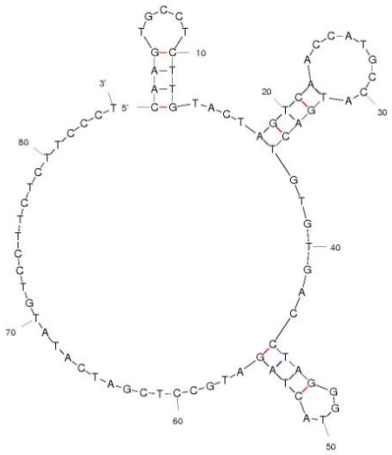

Aptamer 3

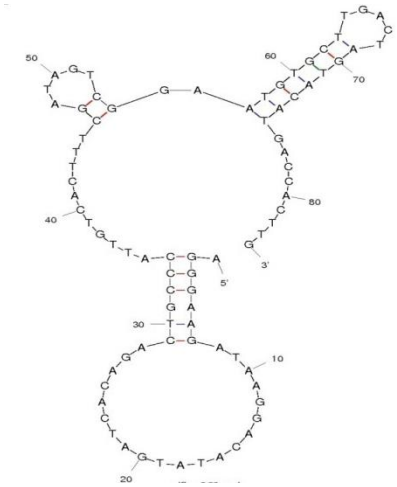

Aptamer 4

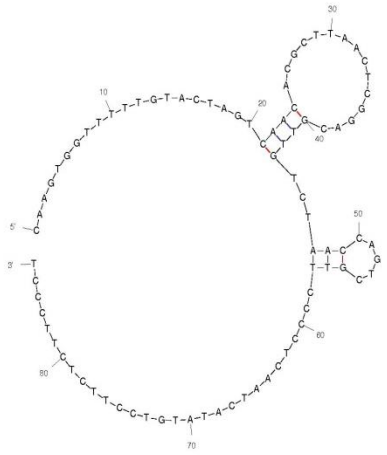

Aptamer 5

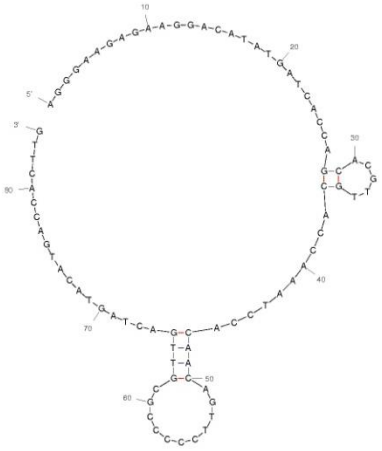

Aptamer 6

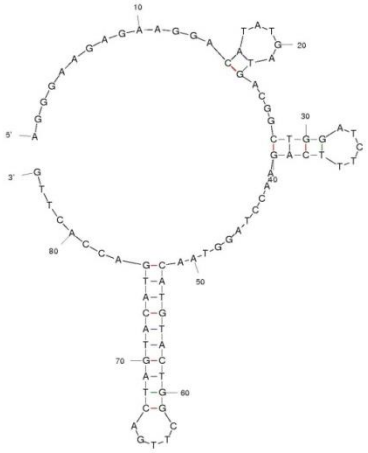

Aptamer 7

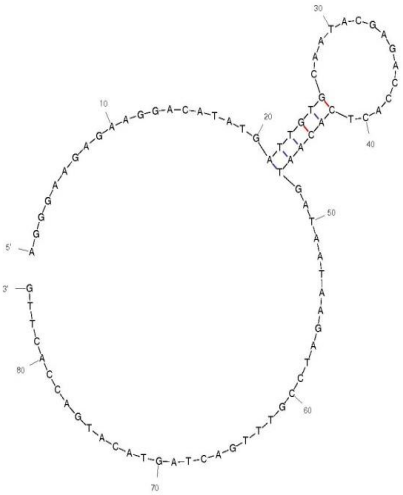

Aptamer 8

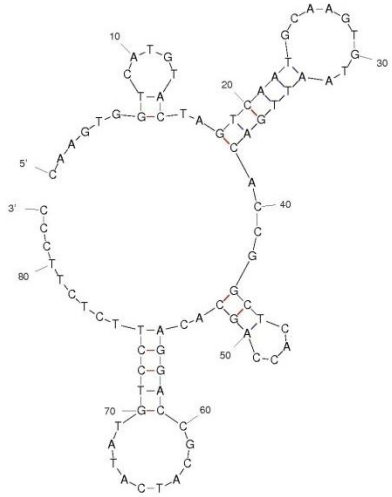

Aptamer 9

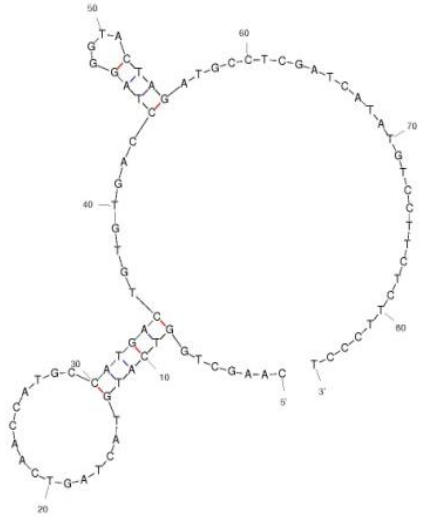

Aptamer 10

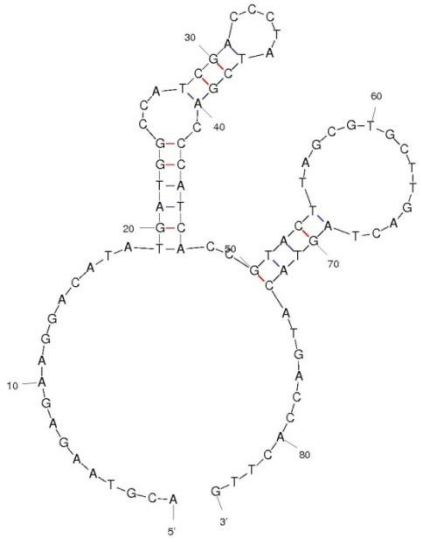

Aptamer 11

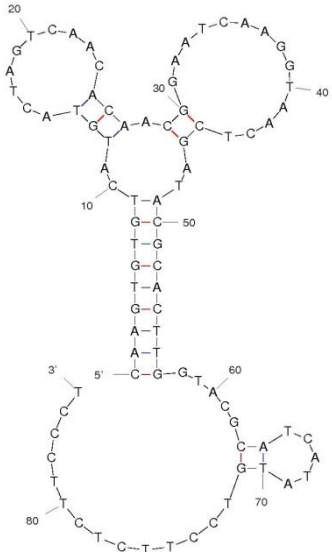

Aptamer 12

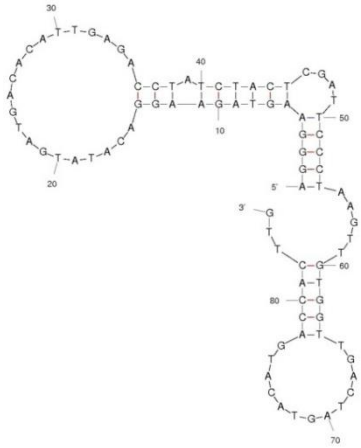

Aptamer 13

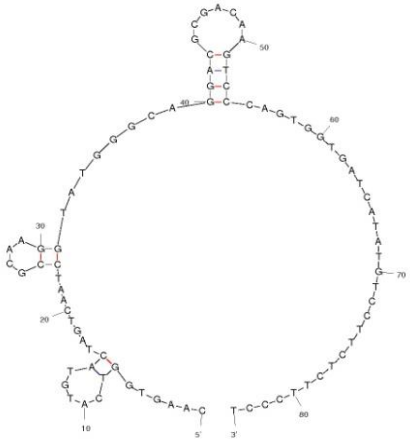

Aptamer 14

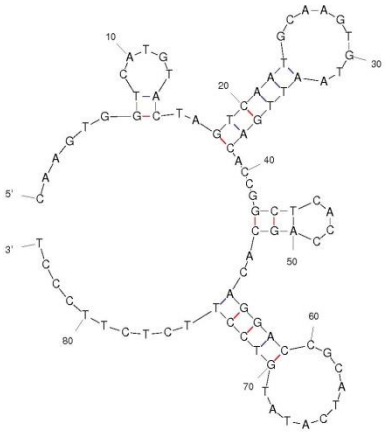

Aptamer 15

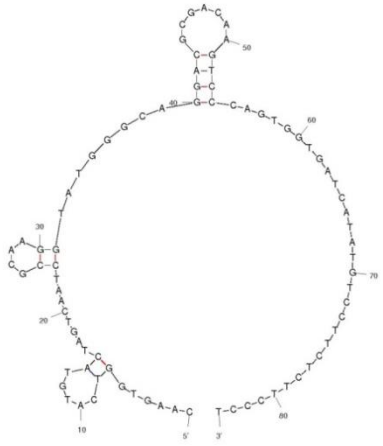

Aptamer 16

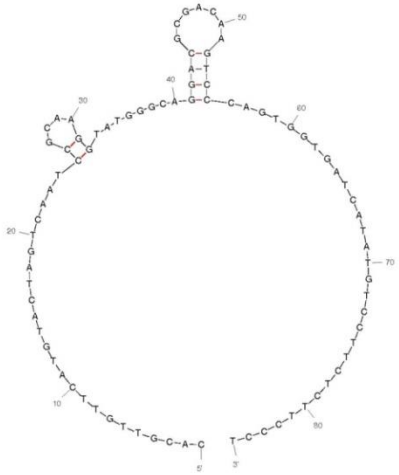

Aptamer 17

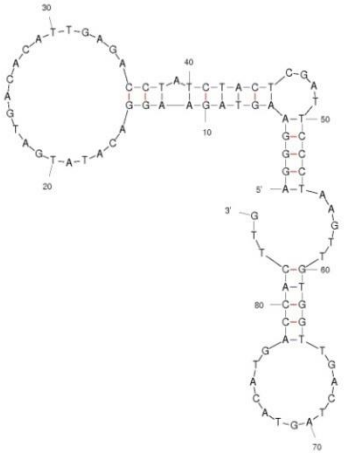

Aptamer 18

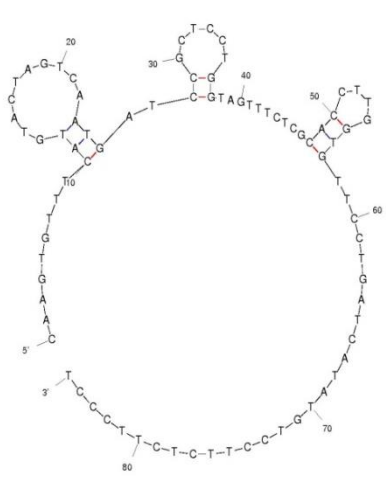

Aptamer 19

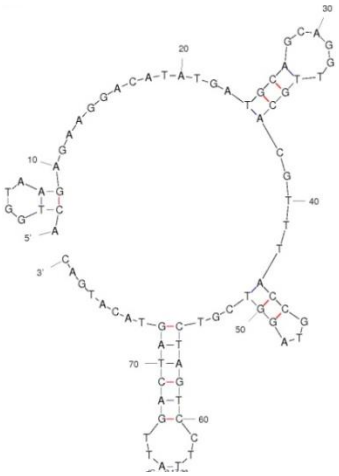

Aptamer 20

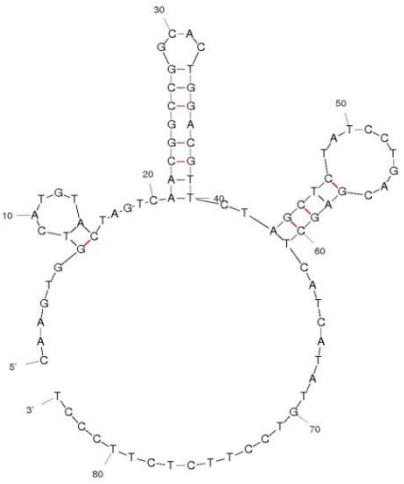

Aptamer 21

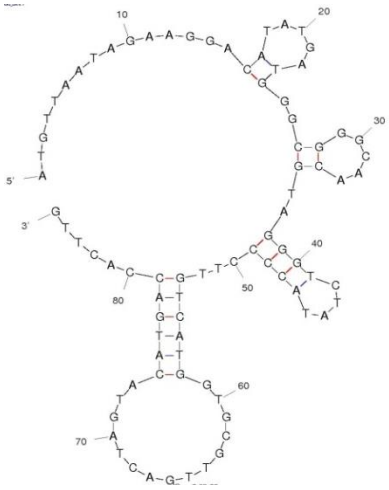

Aptamer 22

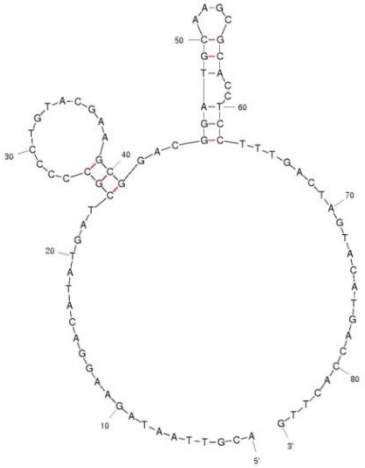

Aptamer 23

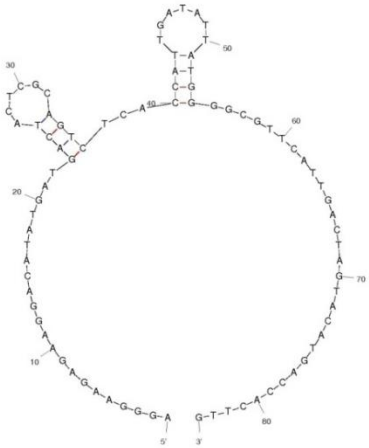

Aptamer 24

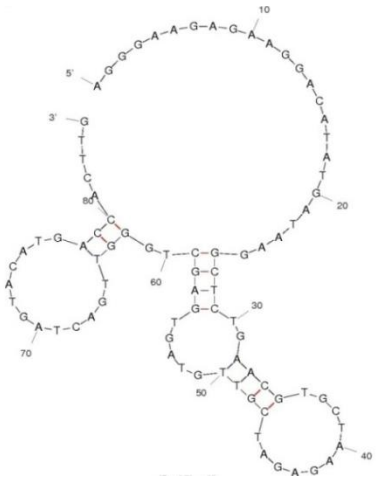

Aptamer 25

Fig.S8. Secondary structures of each aptamer sequence obtained from Mfold web-server.

S3. FTIR for immobilization of aptamer on gold electrodes

FTIR spectra of bare and aptamer immobilized gold electrode is shown in Fig.S9. Bare gold did not show any characteristic FTIR peak. The peaks after immobilization process on gold were obtained at 1820, 1640 and 1420 cm^{-1} due to presence of nucleobases present in aptamer sequence, i.e., C=O stretching in guanine, carbonyl group carbonyl stretching in thymine and in-plane vibrations in cytosine. FTIR peaks were seen at 915, 1090 and 1240cm^{-1} due to asymmetric and symmetric vibrations of phosphate group of phosphodiester deoxyribose backbone, and O-P-O bending. In addition, because of deoxyribose-phosphate of aptamer and C-S bonds involved in thiol linkages, a peak at 810cm^{-1} was acquired. [6, 7] Generation of these peaks on gold confirmed immobilization of aptamer on gold electrode successfully using carbodiimide covalent coupling to layer of aminoethanethiol.

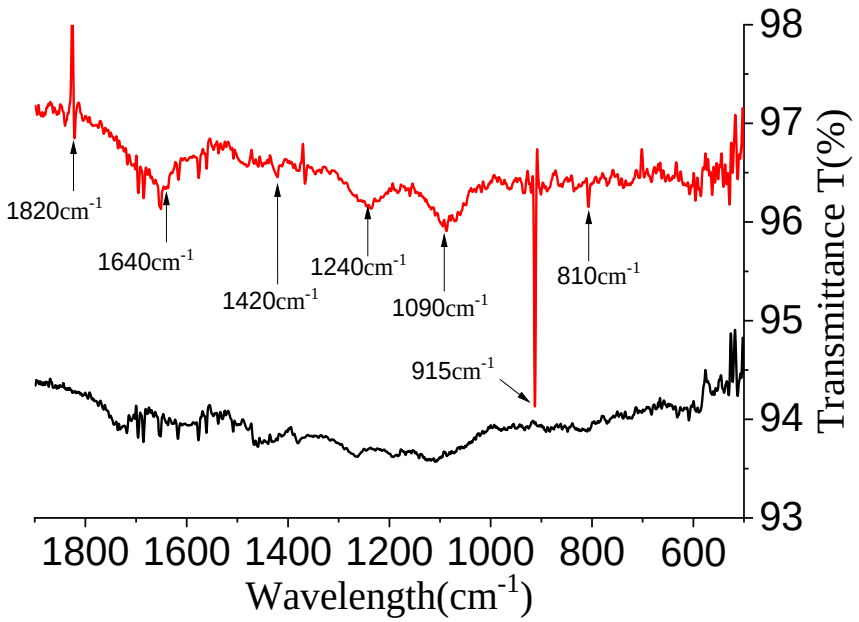

Fig.S9.FTIR spectra of bare gold electrode before (———) and after immobilization (———) of ssDNA aptamer.

Table S2. Linear fit model equation and values obtained with calibration curve in research article Fig.8c

Aptamer 1

Equation	Y =a+b × X		
Adj. R-square	0.99294		
		Value	Standard error
Capacitive component	Intercept	99793.79119	3510.25065
	Slope	2902.37458	118.73139

Aptamer 25

Equation	Y =a+b × X		
Adj. R-square	0.94519		
		Value	Standard error
Capacitive component	Intercept	73742.55441	8993.14089
	Slope	2208	304.18573

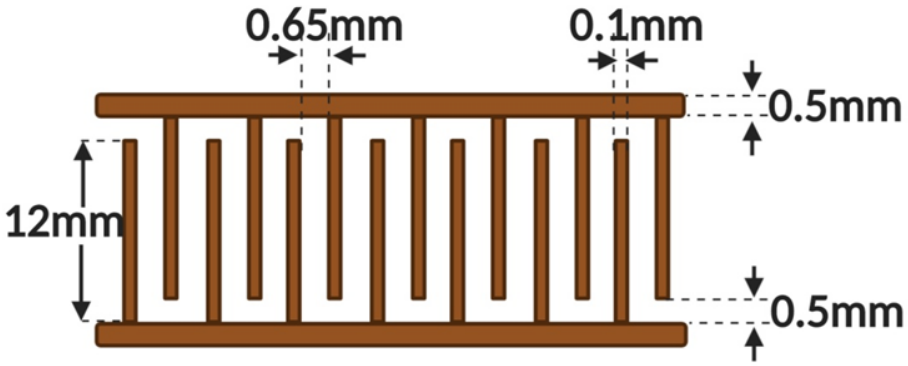

Fig.S10. Dimensions of the interdigitated (IDT) gold electrodes

References

1. B. Samiey and F. Ashoori, Chem. Cent. J.,*2012*, 6, 1.
2. A. Barth, Biochim. Biophys. Acta - Bioenerg.,*2007*, 1767, 1073.
3. N. Chang, B. P., Akil, H. M., Nasir, R. M., Polym. Compos.,*2013*, 1020.doi:10.1002/pc
4. A. Vijayalakshmi, B. Vidyavathy, G. Peramaiyan, and G. Vinitha, J. Solid State Chem.,*2017*, 246, 237.
5. J. Hu, J. Kim, and C. J. Easley, Anal. Methods,*2015*, 7, 7358.
6. M. L. S. Mello and B. C. Vidal, PLoS One,*2012*, 7, 1.
7. S. Radhakrishnan, C. Sumathi, V. Dharuman, and J. Wilson, Anal. Methods,*2013*, 5, 684.